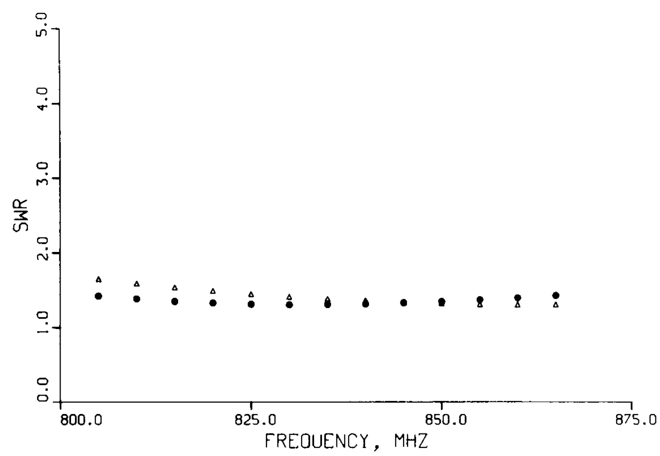

(a)

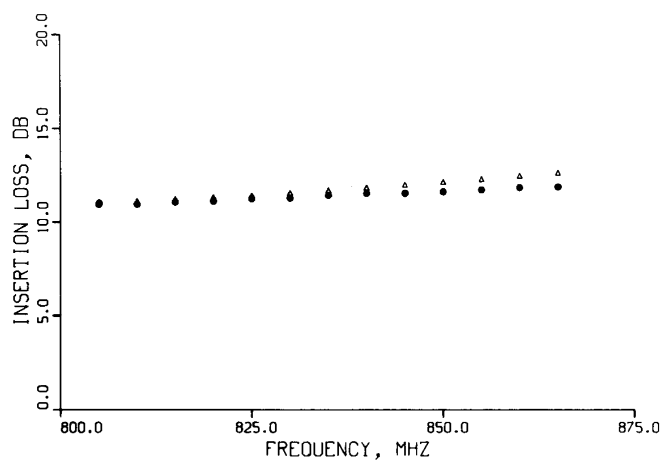

(b)

Fig. 8. Full-scale SWR and insertion loss for 0.0845-m monopole(s). (a) SWR. (b) Insertion loss at 0.12 M. Measured: •••. Calculated: △△△.

ACKNOWLEDGMENT

The author appreciates the help of Ramon Jesch, NBS, who performed all of the network analyzer measurements.

REFERENCES

[1] R. G. FitzGerrell, "Limitations on vertically polarized ground-based antennas as gain standards," *IEEE Trans. Antennas Propagat.*, vol. AP-23, pp. 284-286, Mar. 1975.
[2] ——, "Standard linear antennas, 30 MHz to 1000 MHz," *IEEE Trans. Antennas Propagat.*, vol. AP-34, pp. 1425-1429; Dec. 1986.
[3] E. E. Altshuler, "The traveling-wave linear antenna," *IEEE Trans. Antennas Propagat.*, vol. AP-9, pp. 324-329, July 1961.
[4] R. W. P. King, E. A. Aronson, and C. W. Harrison, Jr., "Determination of the admittance and effective length of cylindrical antennas," *Radio Sci.*, vol. 1 (new series), pp. 835-850, July 1966.
[5] M. T. Ma, *Theory and Application of Antenna Arrays*. New York: Wiley, 1974.
[6] J. H. Richmond, "Monopole antenna on circular disk," *IEEE Trans. Antennas Propagat.*, vol. AP-32, pp. 1282-1287, Dec. 1984.

Comparison of Measured and Calculated Antenna Sidelobe Coupling Loss in the Near Field Using Approximate Far-Field Data

MICHAEL H. FRANCIS, MEMBER, IEEE, AND
CARL F. STUBENRAUCH, SENIOR MEMBER, IEEE

***Abstract*—Computer programs are presently in existence to calculate the coupling loss between two antennas provided that the amplitude and phase of the far field are available. However, for many antennas the complex far field is not known accurately. In such cases it is nevertheless**

Manuscript received December 17, 1986; revised August 24, 1987. This work was supported by the Electromagnetic Compatibility Analysis Center of the Department of Defense.

The authors are with the Electromagnetic Fields Division, National Bureau of Standards, Boulder, CO 80303.

IEEE Log Number 8718774.

possible to specify approximate far fields from a knowledge of the sidelobe level of each antenna along the axis of separation and the electrical size of each antenna. Measurements of near-field coupling loss between two moderately sized microwave antennas were done to determine the effectiveness of using approximate sidelobe level data instead of the detailed far fields. Comparison of the measured and computed coupling indicates that the use of approximate far fields gives an estimate of the coupling loss with an uncertainty of about ±5 dB.

I. Introduction

Two highly efficient computer programs, CUPLNF and CUPLZ, for calculating the coupling loss transverse to and along the separation distance, respectively, between two antennas given the far fields of each antenna were developed some years ago at the National Bureau of Standards (NBS) [1]–[3]. In particular, for antennas arbitrarily oriented and separated in free space, CUPLNF computes the coupling loss at a single frequency (ignoring multiple reflections between antennas) as a function of displacement in a plane transverse to the axis of separation of the antennas. Computation times for coupling loss on a transverse plane over a distance equal to approximately twice the sum of the antenna diameters for antennas hundreds of wavelengths in diameter are a few minutes of CPU time on a typical mainframe computer.

The major limitation of CUPLNF is its requirement for the magnitude and phase of the far field of each antenna within the solid angle mutually subtended by the antennas. In practice, we may not have such detailed information on, for example, the sidelobe far fields to estimate the coupling loss between two cosited antennas in their near field. Often, however, we have some knowledge of the sidelobe levels of the antennas, even if detailed phase and amplitude information is unavailable. Thus a natural and important question to answer is whether this limited information, specifically the sidelobe level of each antenna near its axis of separation, can be used to estimate the antenna coupling loss in the near field. Of course, as the separation distance of the antennas approaches the mutual Rayleigh distance, $(D_T + D_R)^2/\lambda$, the ordinary far-field formula for antenna coupling loss can be used to estimate the coupling loss. It is for separation distances much less than the mutual Rayleigh distance that the far-field formula would not be expected to give accurate estimates for the coupling loss. We set out to see if in this near-field region a program, ENVLP, developed by Francis and Yaghjian [4], will give realistic values of the sidelobe coupling loss (±5 dB) by using sidelobe levels along the axis of separation of the antennas plus the size, separation distance, and reflection coefficients of the antennas.

To estimate the efficacy of ENVLP which uses approximate sidelobe level information instead of detailed far fields, Francis and Yaghjian [4] considered the case of two linearly polarized, uniformly illuminated circular aperture antennas for which the exact far fields are given by a fairly simple analytic expression involving functions no more complicated than the first-order Bessel function. With these hypothetical antennas the exact far fields could be supplied to program CUPLNF to compute the near-field coupling loss. An approximate sidelobe far field was supplied to program ENVLP, and the resulting near-field coupling loss was compared to that from CUPLNF and reasonably accurate agreement found.

II. Formulation of the Problem

Yaghjian [1] showed that the coupling loss between two antennas in free space, neglecting multiple reflections, is given by

$$\frac{b_0'(\mathbf{R}, d)}{a_0} = \frac{-C'}{k} \iint\limits_{K<k} \frac{\mathbf{f}'(-\mathbf{k}) \cdot \mathbf{f}(\mathbf{k}) e^{i\gamma d} e^{i\mathbf{K}\cdot\mathbf{R}}\, d\mathbf{K}}{\gamma} \tag{1}$$

where $C' = 1/(\eta_0 Z_0(1 - \Gamma_0\Gamma_L))$, Γ_0 and Γ_L are the reflection coefficients of the receiving antenna and its passive load, η_0 is the characteristic admittance of the propagated mode in the waveguide feed of the receiving antenna, and Z_0 is the wave impedance of free space. The propagation vector is given by $\mathbf{k} = \mathbf{K} + \gamma\hat{z}$, $\mathbf{K} = k_x\hat{x} + k_y\hat{y}$, $\gamma = (k^2 - K^2)^{1/2}$, $d\mathbf{K}$ is the abbreviation for $dk_x dk_y$, and $(\mathbf{R}, z = d)$ give the position of the coordinate system fixed to the receiving antenna with respect to the (x, y, z) coordinate system fixed to the transmitting antenna (see Fig. 1). The functions $\mathbf{f}$ and $\mathbf{f}'$ are the complex electric far-field patterns of the transmitting and receiving antennas, respectively, without the presence of the other, a_0 is the amplitude of the wave incident on the transmitting antenna, and b_0' is the amplitude of the wave emergent from the receiving antenna. (Formula (1) assumes the receiving antenna is reciprocal; however, for nonreciprocal receiving antennas the receiving spectrum is used instead of $\mathbf{f}'$.) Yaghjian [1] also showed that for most practical situations the integration range in (1) could be limited to about $K/k < (D_T + D_R)/2d$ for $R \approx 0$ provided that $(D_T + D_R)/2 < d < (D_T + D_R)^2/\lambda$. D_T is the diameter of the smallest sphere which circumscribes the transmitting antenna, and D_R is the smallest sphere which circumscribes the receiving antenna. If D_T or D_R is less than twice the wavelength, D_T or D_R is replaced by 2λ. For coupling loss in the transverse plane over the range $-(D_T + D_R) < R < (D_T + D_R)$ the integration range should be approximately doubled [1]. To save computer time we hold $y = 0$ while varying x and hold $x = 0$ while varying y.

Some situations arise where detailed information of the far fields $(\mathbf{f}, \mathbf{f}')$ is lacking, and an estimate of the coupling loss between two antennas is desirable. Therefore, to have a method of approximating the coupling loss and, in particular, of finding a good estimate of the maximum coupling loss between two antennas along the general direction of the separation axis is also desirable.

III. The Approximate Far Field

The approximation used in the ENVLP program for the far field is a general approximation that can be made for a large class of coupled antennas. For this approximation we replace $\mathbf{f}'(-\mathbf{k})\cdot\mathbf{f}(\mathbf{k})$ in the sidelobe region by

$$A_{T\,\max} \cos(k_x a_T) \cos(k_y a_T) A_{R\,\max} \cos(k_x a_R) \cos(k_y a_R) \tag{2}$$

where a_T and a_R are the radii of the radiating apertures of the transmitting and receiving antennas, respectively, $k_x = k \sin\theta \cos\phi$, $k_y = k \sin\theta \sin\phi$, and $A_{T\,\max}$ and $A_{R\,\max}$ are the magnitudes of the approximate electric far fields in the direction of the separation axis (in absolute SI units). They are given in [4] as

$$A_{T\,\max} = (\eta_{0T} Z_0 (1 - |\Gamma_{0T}|^2))^{1/2} 10^{((G_T - S_T)/20)} \tag{3a}$$

and

$$A_{R\,\max} = (\eta_{0R} Z_0 (1 - |\Gamma_{0R}|^2))^{1/2} 10^{((G_R - S_R)/20)} \tag{3b}$$

where G_T, G_R are the gains of the transmitting and receiving antennas, respectively, and S_T, S_R are the relative sidelobe levels in the direction of the separation axis of the transmitting and receiving antennas, respectively.

We have chosen this approximation because for many antennas the far sidelobe region of the far-field pattern is predominantly caused by diffraction from edge points of the antenna. These edge points are usually separated by a distance of approximately an antenna diameter, and this leads to a sidelobe pattern which has a null approximately every $\lambda/2a$ rad as many hypothetical and measured far-field patterns confirm (e.g., Johnson *et al.* [5], and Newell and Crawford [6]). Polarization matching of the antennas is also assumed; this tends to lead to an upper bound.

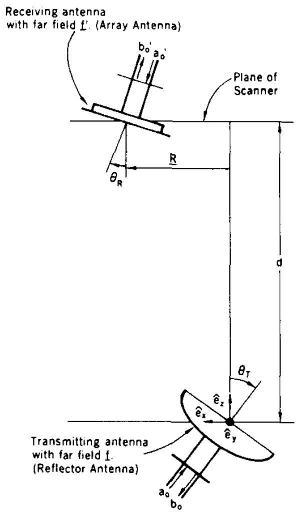

Fig. 1. Schematic of two arbitrarily oriented and separated antennas. Coupling loss is $b_0'(\mathbf{R}, d)/a_0$. For transverse displacement, d is held constant; for radial displacement, $\mathbf{R} = 0$. Also shown are simplified coordinates used for coupling loss measurements.

Using (2) in (1) ENVLP computes the coupling loss along a line segment perpendicular to the separation axis. From this ENVLP determines the maximum coupling loss along the line segment and the rms mean of the coupling loss along the line segment. In [4] it is concluded from the hypothetical test case that the actual coupling loss of the antennas along the separation axis should in most cases lie below the computed maximum coupling loss and be within ± 5 dB of the computed rms mean coupling loss (plus the uncertainty of the sidelobe levels).

IV. Measurement Procedure

To verify the efficacy of the coupling loss formulation of ENVLP experimentally, coupling loss between two antennas was measured using the National Bureau of Standards near-field scanner, which allows precise determination of the relative orientation of two antennas. The first antenna was a 1.2-m reflector antenna having a power gain of about 30 dB and a half-power beamwidth of about 4.5°. The second antenna was a 25-element microstrip array with a power gain of about 22 dB and a half-power beamwidth of about 15°.

The microstrip array was mounted on the x-y positioner of the near-field scanner. Two wedges were also available to allow the microstrip array to be rotated about the vertical axis by angles of 21.6° or 30.3°. The reflector antenna was mounted on an azimuth positioner.

In all cases the polarization vectors of the antennas were oriented in the y direction. The measurements were made for coupling loss as a function of θ_T and θ_R, where θ_T and θ_R are the angles by which the transmitting or receiving antenna boresight direction is rotated with respect to the common coordinate system as illustrated in Fig. 1.

V. Results and Comparisons

Five orientations of the two antennas were chosen to compare the results of ENVLP to experimental results. These orientations are defined in Table I. For the first two orientations all criteria as specified in [4] are met. For the third and fourth orientations of Table I, coupling loss involves parts of the main beams and, for the last orientation, the antennas are directly facing each other, and thus coupling loss involves mostly the main beams.

The results from ENVLP are compared to the experimental results in Table II. The computed maximum is indeed an upper bound and the computed rms mean falls within the stated ± 5 dB uncertainty for all cases except orientation 5. The results of orientation 5 are not within the stated uncertainty because the coupling occurs through the main beams, where (2) is a poor approximation, rather than through the sidelobes of the antennas.

At first, it may appear surprising that the results for orientation 3 fall within the uncertainties of ENVLP since it involves the main beam of the microstrip array. A careful examination of the microstrip far-field pattern and the angle subtended by the dish indicates that only about 11 percent of the main beam of the microstrip array sees the dish and the maximum power level of that part of the main beam is only twice the maximum sidelobe level. Thus case 3 falls within the expected uncertainty of ENVLP.

For case 4, however, the dish sees the microstrip only through its main beam, and thus it is merely fortuitous that the measured coupling loss lies within the expected uncertainty. In general, ENVLP should not be used to calculate the coupling loss between antennas if more than about 15 percent of the main beam of one antenna is subtended by the other antenna.

Finally, we should mention that when one or both antennas are reflector antennas, the approximation (2), on which the computer program ENVLP is based, assumes that the subtended sidelobes of each reflector antenna are determined predominantly by the reflector fields. If, however, spillover from a reflector feed dominates the subtended sidelobe region, the radius of the feed should be used in (2) rather than the radius of the reflector.

TABLE I
ORIENTATIONS STUDIED FOR ENVLP

Orientation	θ_T (deg)	θ_R (deg)
1	30	−30.3
2	20	−30.3
3	20	−21.6
4	0	−21.6
5	0	0

Separation (all cases)	4.0 m
Frequency (all cases)	4.0 GHz
Radius of microstrip array	0.15 m
Radius of reflector antenna	0.61 m

TABLE II
COUPLING LOSS RESULTS FROM ENVLP AND EXPERIMENT

Orientation	RMS Mean (dB)	Maximum (dB)	Experimental Result (dB)
1	−65.51	−59.14	−61.58
2	−53.51	−47.14	−57.91
3	−49.51	−43.14	−50.72
4	−31.48	−25.12	−28.50
5	−21.49	−15.12	−12.57

Acknowledgment

The authors wish to thank Arthur D. Yaghjian of the Rome Air Development Center, Hanscom Air Force Base, MA, and Allen C. Newell of NBS for consultation, and Douglas P. Kremer and Douglas T. Tamura for performing the measurements.

References

[1] A. D. Yaghjian, "Efficient computation of antenna coupling and fields within the near-field region," *IEEE Trans. Antennas Propagat.*, vol. AP-34, pp. 113–128, Jan. 1982.

[2] C. F. Stubenrauch and A. D. Yaghjian, "Determination of coupling loss between co-sited microwave antennas and calculation of near-zone electric field," Nat. Bur. Stand (US), NBSIR 80-1620, June 1981.
[3] C. F. Stubenrauch and M. H. Francis, "Comparison of measured and calculated coupling loss in the near field between microwave antennas," *IEEE Trans. Antennas Propagat.*, vol. AP-34, pp. 952–955, July 1986.
[4] M. H. Francis and A. D. Yaghjian, "Computation of antenna sidelobe coupling in the near field using approximate far-field data," Nat. Bur. Stand. (US), NBSIR 82-1674, Aug. 1982.
[5] R. C. Johnson, H. A. Ecker, and J. S. Hollis, "Determination of far-field patterns from near-field measurements," *Proc. IEEE*, vol. 61, pp. 1668–1694, Dec. 1973.
[6] A. C. Newell and M. L. Crawford, "Planar near-field measurements on high performance array antennas," Nat. Bur. Stand. (US), NBSIR 74-380, July 1974.

Interpolation Methods for Shaped Reflector Analysis

VICTOR GALINDO-ISRAEL, WILLIAM A. IMBRIALE, MEMBER, IEEE, YAHYA RAHMAT-SAMII, FELLOW, IEEE, AND THAVATH VERUTTIPONG, MEMBER, IEEE

Abstract—**It is often required to find "smooth" analytic representations for antenna reflector surfaces which are prescribed only by discretized data obtained by various synthesis methods. Frequently, the data are distributed in a nonuniform grid and contain noise. The "smoothness" required is to the first derivative for physical optics diffraction analysis and to the second derivative for geometrical theory of diffraction (GTD) analysis. Furthermore, the GTD analysis approach requires a surface description which returns data very rapidly since a search procedure is used to find the spectral point of reflection. Two methods of interpolation, the global and the local methods, are discussed herein. They each have advantages and disadvantages—usually complementary. These characteristics are discussed and examples are presented.**

I. Introduction

The diffraction analysis of reflector surfaces which are described only at a *discrete* set of locations usually leads to the requirement of an *interpolation* to determine the surface characteristics over a continum of locations. Such discretized surface descriptions can come about from a set of point measurements, for example. Another common source of such a description is the dual offset shaped reflector synthesis [3]–[5], which may involve numerical difference type solutions over a discretized field.

The physical optics analysis of a reflector antenna requires an accurate description of the point characteristics (e.g., $[x, y, z]$ or $[r, \theta, \phi]$) of the surface. It also requires a (less stringently) accurate description of the slopes (e.g., $[z_x, z_y]$[1] or $[r_\theta, r_\phi]$) at the same points. The geometrical theory of diffraction (GTD) analysis requires, further, an accurate knowledge of the second derivatives at the same points. The second derivatives provide the scattered amplitude for both the GO and the diffraction parts of GTD. Hence the GTD analysis of shaped reflectors with discretized raw data requires an accurate and often time-consuming interpolation process.

In dual reflector antennas, it is usually desirable to analyze the subreflector by GTD since many more near-zone observation points are required on the main reflector than far-field observation points scattered from the main reflector. We analyze the main reflector (including the diffraction effect) by the Jacobi–Bessel method [7]–[9]. The interpolation techniques to be described are applicable to both reflectors, but we will describe results found for a shaped subreflector synthesized for high gain (when used with a paired shaped main reflector).

High gain shaped subreflectors represent a more than average difficult surface to describe because the surface curves rapidly and often possesses inflection points [3]–[10]. A profile description of such a dual reflector is shown in Fig. 1. Also illustrated are the projected discretized raw data locations (on the $[\theta, \phi]$ plane) at equal $(\Delta\theta, \Delta\phi)$ increments. In some synthesis methods [3], the raw data consist of r, r_θ, and r_ϕ at each (θ, ϕ) discretized location. However, the derivative data of at least one derivative (in [3], the r_ϕ derivative) are potentially unstable since they are computed by difference techniques which do not permit very small increments.

A method for evaluating the accuracy and stability of a surface description is to compute the "distance" function derivatives D_ϕ and $D_{\phi\phi}$. The distance D is the distance from the source to a point on the reflector and then to the observation point. When D is a minimum (Fermat's principle), we have a GO or an edge diffraction spectral point. In our evaluation method, we allow the point on the subreflector to vary in position with ϕ (θ fixed). Usually we take $\theta = \theta_{\max}$ along the edge of the reflector, although all θ values should be evaluated.

The results for a particular set of raw data [10] are shown in Fig. 2. Note the erratic second derivative behavior (one of at least two diffraction spectral points are at the (θ, ϕ) point at which $D_\phi = 0$).

The actual surfaces will appear "rough" as the distance function appears in Figs. 2 and 3, except that the roughness is difficult to observe unless the surface is greatly magnified. The distance function D and the distance derivatives are more directly significant to computations (by GTD in particular).

II. Global Interpolation

A global interpolation representation is a closed-form or series expression valid over the entire surface. The coefficients of a series expression are found by an integration[2] of all of the raw data. Since the number of coefficients used to describe the surface are much fewer than the number of raw data points, the integration effectively provides a smoothing of the raw data.

For example, the Jacobi polynomial–sinusoidal expansion [7], [11] was found to provide a fast converging representation of the offset shaped subreflector discussed. The representation is

$$r(\theta, \phi)=\sum_{n=0}^{N-1}\sum_{m=0}^{M-1} a^{\overset{e}{o}}_{mn} F^{n}_{m}(\theta) \begin{Bmatrix}\cos n\phi \\ \sin n\phi\end{Bmatrix}$$

Manuscript received March 19, 1987; revised September 24, 1987. This work was carried out by the Jet Propulsion Laboratory, California Institute of Technology, under contract with the National Aeronautics and Space Administration.

The authors are with the Jet Propulsion Laboratory, California Institute of Technology, 4800 Oak Grove Drive, Pasadena, CA 91109.

IEEE Log Number 8718762.

[1] Where $\partial z/\partial x = z_x$.

[2] Any suitable integration method can be used, dependent upon the distribution of the raw data. For ordered but otherwise unequally spaced raw data, a trapezoid (triangular facet) two-dimensional integration can be used.

0018-926X/88/0300-0441$01.00